

available at www.sciencedirect.comwww.elsevier.com/locate/brainres

**BRAIN
RESEARCH**

Research Report

Layer IV of the primary somatosensory cortex has the highest complexity under anesthesia and cortical complexity is modulated by specific thalamic inputs

Zi-Hao Wang^{c,d}, Ming-Hua Chang^a, Jenq-Wei Yang^a, Jyh-Jang Sun^a,
Hoong-Chien Lee^b, Bai-Chuang Shyu^{a,*}

^aInstitute of Biomedical Sciences, Academia Sinica, Taipei 11529, Taiwan, ROC

^bDepartment of Physics and Institute of Biophysics, National Central University, Chungli 320, Taiwan, ROC

^cComputing Centre, Academia Sinica, Taipei 11529, Taiwan, ROC

^dInstitute of Neuroinformatics, ETHZ/UNIZH, Winterthurerstrasse 190, 8057 Zürich, Switzerland

ARTICLE INFO

Article history:

Accepted 18 January 2006

Available online 24 February 2006

Keywords:

Cortical layer

Correlation dimension

Fractal exponent

Nonlinear dynamic

Power spectrum

ABSTRACT

The system complexity, as calculated from correlation dimension, embedded in each layer and its modulation by specific inputs and general excitatory state are not yet known. The aims of present study were to estimate the system complexity across the cortical layers by analyzing intracortical EEG signals using a nonlinear analytical method, and to identify how layer-related complexity varies with the alteration of thalamic input and brain state. Male Sprague–Dawley rats were anesthetized under 1% halothane. Sixteen channels of evoked or spontaneous EEG signals were recorded simultaneously across the six cortical layers in the somatosensory cortex with a single Michigan probe. The system complexity was assessed by computing correlation dimension, D_2 , based on the Nonlinear Time Series Analysis data analysis program. Cortical layer IV exhibited a D_2 value, 3.24, that was significantly higher than that of the other cortical layers. The D_2 values in layers IV and II/III were significantly reduced after reversible deactivation of the ventral posterior lateral thalamic nucleus. D_2 decreased with increases in administered halothane concentration from 0.75% to 2.0%, particularly in layer IV. The present findings suggest that cortical layer IV maintains a higher complexity than the other layers and that the complexity of the mid-cortical layers is subject to regulation from specific thalamic inputs and more sensitive to changes in the general state of brain excitation.

© 2006 Elsevier B.V. All rights reserved.

1. Introduction

Nonlinearity has been found to be embedded in brain dynamic processes from activities at the microscopic cellular level to macroscopic sets of connections at the cortical level (Babloyantz and Destexhe, 1986; Theiler, 1995). As a result,

quantitative analysis of electroencephalogram (EEG) data by nonlinear dynamical methods has often been used to elucidate the underlying dynamics of neuronal processes. The scalar EEG time series in high dimensional Euclidean space can be reconstructed by the nonlinear time series analysis method (NTSA) (Kantz and Schreiber, 1997).

* Corresponding author. Fax: +886 2 2782 9224.

E-mail address: bmbai@gate.sinica.edu.tw (B.-C. Shyu).

Employing the embedding theory (Takens, 1981), NTSA can be used to extract from EEG data quantities such as the largest Lyapunov exponent and correlation dimension (D_2) which are quantitative indices of the brain's electrical activity (Jeong et al., 1998; Kotini and Anninos, 2002; Pereda et al., 1999). D_2 is one of the characteristic invariants of nonlinear dynamics that can give a good measure of complexity of the underlying attractor in a dynamic system (Anokhin et al., 1996). Such dimensional complexity can be used to quantitatively characterize EEG signals: the greater the dimensionality, the more complex the signals. Therefore, the correlation dimension may reflect the complexity of EEG dynamics and, probably the complexity of neurophysiological processes generating the EEG signals. The better understanding of principles that govern dynamics and complexity of EEG signals may help to reveal the specificity of different physiological and pathological states of the brain.

The NTSA technique has been used successfully to predict physiological brain states (Babloyantz et al., 1985) and to aide in the diagnosis of pathological brain states including epilepsy (Ferri et al., 2001; Lehnertz, 1999; Theiler, 1995), Parkinson's disease (Stam et al., 1995), Alzheimer's (Jeong et al., 1998; Van Cappellen van Walsum et al., 2003) and schizophrenia (Lee et al., 2001). The EEG data analyzed in nonlinearity studies have generally been from scalp or cortical surface recordings. There was a report of an intra-cortical deep EEG study using a nonlinear method (Van der Heyden et al., 1999), but it did not include a comparison of the complexities across the cortical layers.

Cytoarchitectural studies have demonstrated that the neocortex consists of six distinct layers that are parallel to the cortical surface. In the vertical dimension, neurons are organized into groups that are linked synaptically across the horizontal layers. Each of these vertically oriented narrow chains of neurons, called minicolumns, is regarded as the basic unit of the neocortex (Mountcastle, 1997). Minicolumns are further connected by short-range horizontal connections and organized into functional modules of a higher order called cortical columns which are formed by neurons with similar physiological properties (Mountcastle, 1997). This modular organization is a widely recognized design principle for the structure and function of the brain (Jones, 2000; Mountcastle, 2003). The cortical column is a complex processing and distributing unit that links multiple inputs to multiple outputs via overlapping internal processing chains. All neurons inside a column are tightly linked with connections that extend to adjacent columns and distant columns, and into subcortical areas, particularly the thalamus. Cortical layer IV receives the major inputs from the thalamus and transmits signals to the supragranular and infragranular parts of the column. The thalamus receives sensory information from the periphery and all parts of the cortex and works together with the cerebral cortex to create a feedback circuit by passing information from the infragranular cells of the cortex to the thalamus and then back to the layer IV cells of the cortex (Scannell et al., 1999). The reciprocal connections within the cortico-thalamo-cortical system have been proposed to underlie gate/gain mechanisms at

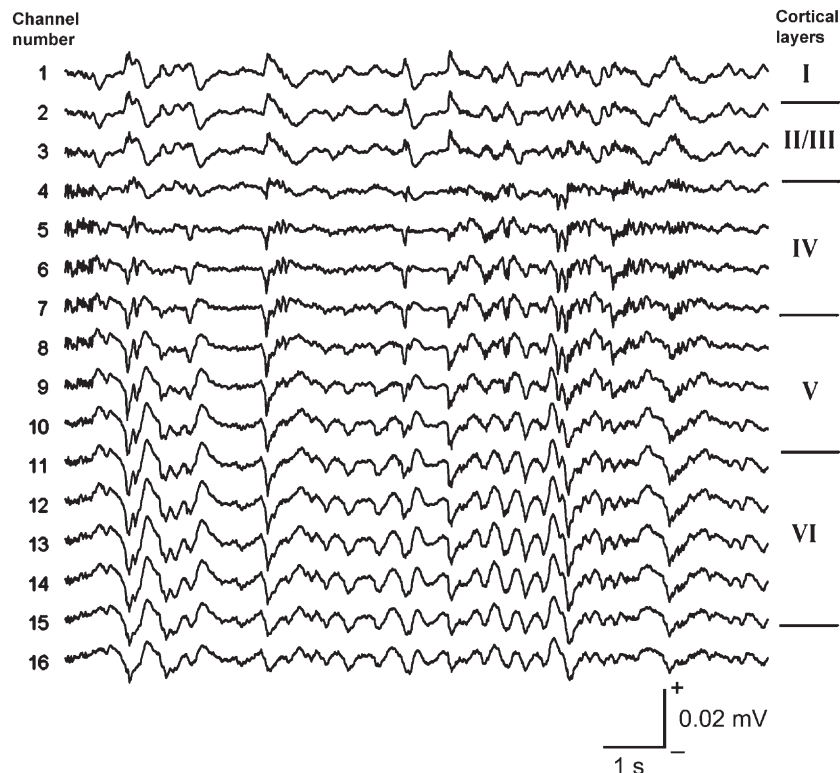


Fig. 1 – Spontaneous EEG recordings in 16 channels (from cortical layers I to VI, labeled at right) of an epoch extracted from 160-s records.

an early stage of sensory information processing (Crick and Koch, 1998). It remains to be determined what portion of the changes in system complexity of neuronal information flow is processed in this basic cortical module. Thus, we hypothesize that correlation dimension may differ in different cortical layers, and that the complexity in the cortical layers may be subject to change in general excitatory states and more specifically to the thalamic input drives.

The primary aim of present study was to investigate the complexity changes across the cortical layers in the primary somatosensory cortex of rats and further to investigate factors that may influence cortical layer dependent complexity, namely the level of brain excitatory state and thalamic input. EEGs from cortical layers I to VI were recorded simultaneously and analyzed with NTSA method. The averaged D_2 and scaling exponent in double log scale spectrum of each layer were recorded to elucidate the neuronal activities within cortical columns. Intra-cortical complexities associated with different brain states were evaluated by varying anesthesia levels. The influences of specific thalamic inputs on system complexity were investigated by studying the effects of reversibly deactivating the ventral posterior lateral (VPL) thalamic nucleus.

2. Results

To evaluate system nonlinearity, 9 sets of multichannel EEG signals from 5 different rats at rest were obtained. The D_2 values of the original and corresponding surrogate data were calculated from the TISEAN for each channel. The mean and SEM. of the respective D_2 of all sampled data were 2.88 ± 0.03 (original) and the 2.96 ± 0.03 (surrogate). Paired *t* tests revealed a significant difference between these two groups with ($P < 0.001$).

2.1. Spontaneous and evoked activity across the cortical layers

Spontaneous complex brain activities in the primary somatosensory cortex as revealed by multichannel EEG recordings were observed. An example of an 8-s epoch of simultaneous EEG time series recordings in 16 channels is shown in Fig. 1. Similar EEG oscillatory waves but of varied frequency, amplitude, phase and polarity were observed across the different channels. Oscillations with fast frequencies were noted in some segments of EEG recordings. The approximate cortical layer distributions of each recording channel, as determined by histological observation, are labeled in the right column of Fig. 1. The spontaneous EEG in the superficial layers (I and II/III) exhibited many biphasic (positive/negative) potentials. The potentials of the deeper layers, from layer IV down, tended to change their polarity. A representative example of the CSD profiles of evoked field potentials is shown in Fig. 2. The post-stimulus latency of the earliest sink current in layer IV was about 15 ms. Sink currents with longer latencies were distributed in superficial and deep layers. It appeared that

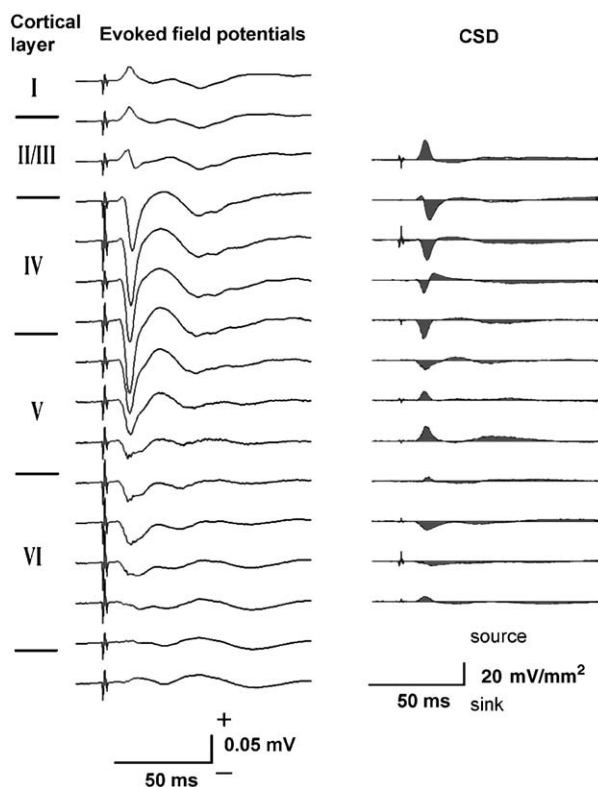


Fig. 2 – An example of multichannel recordings of evoked potentials and their CSD profiles. The field potentials showed evoked positive response in the superficial layers (I, II/III), but potentials reversed to negativity from layer IV. The CSD in layer IV exhibited the earliest sink current after electrical stimulation. The downward direction of the current is the sink and the upward direction is the source.

activated synaptic events started from layer IV and then traveled up to layers II and III and down to layers V and VI.

2.2. Complexities in different cortical layers

The 16 channel EEG revealed low complexity with the averaged correlation dimension, D_2 , ranging from 2.23 to 3.65 in five animals. A representative example of D_2 changes across recording channels is shown in Fig. 3a. D_2 was maximal in recording channel 5. The correlation dimension D_2 quantified the geometrical complexity in the phase portrait. The topological patterns of the delay phase diagrams measured from channels representing the different cortical layers differed among the channels (Fig. 3b). The channel numbers were assigned such that they corresponded to the same cortical layers across animals, enabling mean D_2 values to be calculated and analyzed (Fig. 3c). Cortical layer IV had the largest mean D_2 value (3.24 ± 0.03 , $n = 5$), which implies that it has the most complex dynamical portrait in phase space. ANOVA and post hoc testing showed that the D_2 of layer IV was significantly different from that of all the other layers. The D_2 values of layers II/III and layer V were similar. The D_2 value of cortical layer VI differed significantly from all other layers except layer I (Table 1).

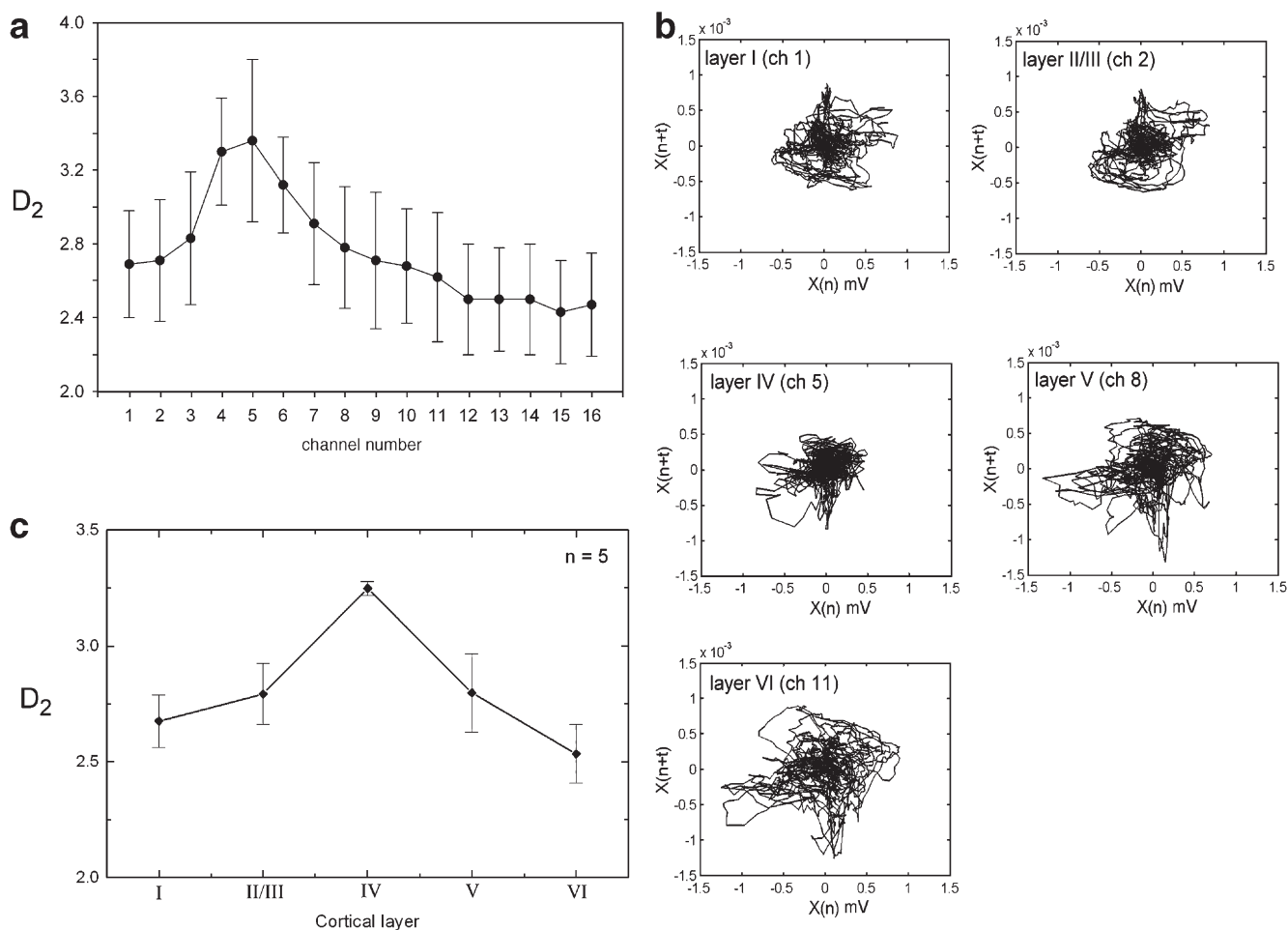


Fig. 3 – Correlation dimension and phase portrait in different channels or different cortical layers. (a) The averaged correlation dimension on each channel was obtained from 20 subsets, 8 s, per rat. (b) The time delay ($t = 80$ ms) phase portraits of channels representing the different layers showed different geometric patterns. (c) The D_2 of each cortical layer was averaged from 5 rats. Note that the D_2 of layer IV exhibited the largest value.

2.3. Power spectrum analysis

The linear scale power spectrums of the channels representing the different cortical layers and typical examples are shown in Figs. 4a–e. Differences of spectrum distribution among the layers were observed. The averaged power spectrum densities (in Fig. 4g) of the low frequency, alpha, beta, and gamma bands in each cortical layer were calculated to illustrate the distinctions among layers. In layer IV the low frequency component decreased dramati-

cally, while the beta and gamma components increased. The power spectrum in log–log scale showed the scaling nature of the EEG. The spectra range of 2–70 Hz presented the power law $1/f^{-\beta}$ dependence; an example from layer IV (channel 5) is shown in Fig. 4f. The scaling exponent β was obtained from a linear regression fit within this frequency range. The fitted slope for cortical layer IV was the lowest (0.95 ± 0.05) of all the layers, and the EEG of cortical layer IV revealed more low amplitude and high frequency fluctuations than that of the other layers. The decreasing

Table 1 – D_2 and β in different cortical layers					
	Layer I	Layers II/III	Layer IV	Layer V	Layer VI
D_2	$2.67 \pm 0.11^*$	$2.79 \pm 0.13^{a,*}$	3.24 ± 0.03^a	$2.79 \pm 0.16^{a,*}$	$2.53 \pm 0.12^*$
β	$1.24 \pm 0.03^*$	$1.15 \pm 0.05^{b,*}$	0.95 ± 0.05	$1.14 \pm 0.06^{c,*}$	$1.30 \pm 0.04^*$

Data presented as means \pm SEM ($n = 5$).
^a $P < 0.05$, compared with D_2 in layer VI.
^b $P < 0.05$, compared with D_2 in layer VI.
^c $P < 0.01$, compared with D_2 in layer VI.
^{*} $P < 0.01$, compared with D_2 in layer IV.

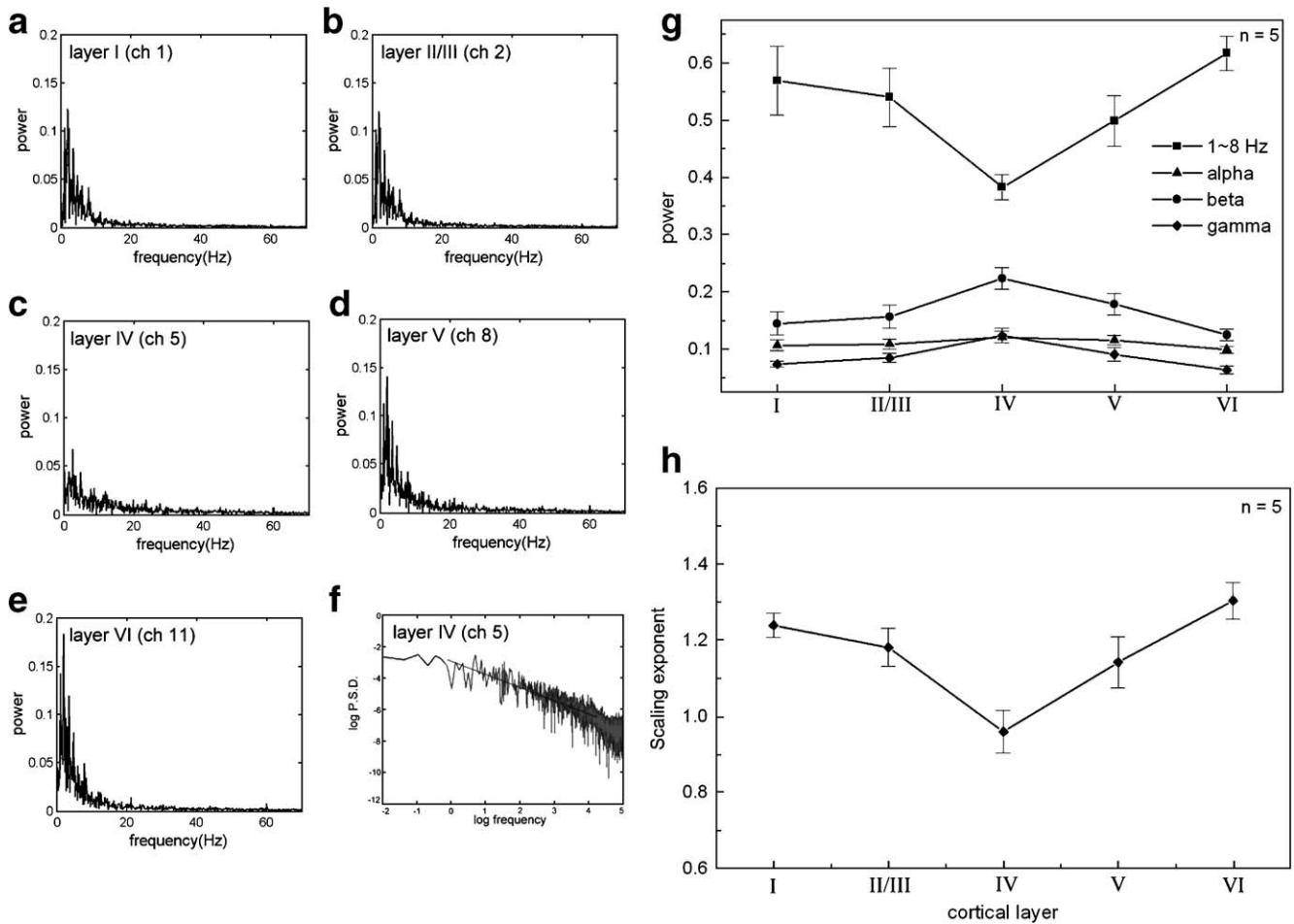


Fig. 4 – Power spectrum and scaling exponent in different channels or cortical layers. (a–e) The Fast Fourier Transform power spectrums of channels representing the different cortical layers. (f) In the log–log scale, the power spectrum density showed the power law character as demonstrated in one channel in cortical layer VI. (g) The power spectrum densities of low frequency (square), alpha (triangle), beta (circle), and gamma (diamond) bands exhibited cortical layer dependence. (h) The cortical layer dependence of scaling exponent. The power density in layer IV decreasing in the low frequency band but increasing in the other bands (shown in Fig. 3b) made the fractal exponent small.

low frequency component with increasing high frequency components Fig. 4g) made the scaling exponent β small for layer IV, and consequently significantly different from the β 's of all the other layers (Table 1). A negative linear correlation between D_2 and β from these data was found with a correlation coefficient of 0.73 (Fig. 5; $n = 5$).

2.4. Effects of depth of anesthesia

The physiological effects of anesthesia level (0.75%, 1% or 2% halothane) were evidenced by the electrically-evoked sink source current profiles (Fig. 6a). The amplitudes of the earliest sink in layer IV were -20.33 ± -7.62 , -15.84 ± -4.19 and -12.54 ± -3.12 mV/mm² in 0.75%, 1% and 2% halothane, respectively. The peak latency of the evoked sink current with 2% halothane was significantly longer than at 0.75% halothane (17.27 ± 0.67 versus 15.89 ± 0.54 ms). As depth of anesthesia increased, the D_2 decreased monotonically and the maximum D_2 shifted to superficial layers (Fig. 6b). The D_2 of each channel with 0.75% halothane were treated as

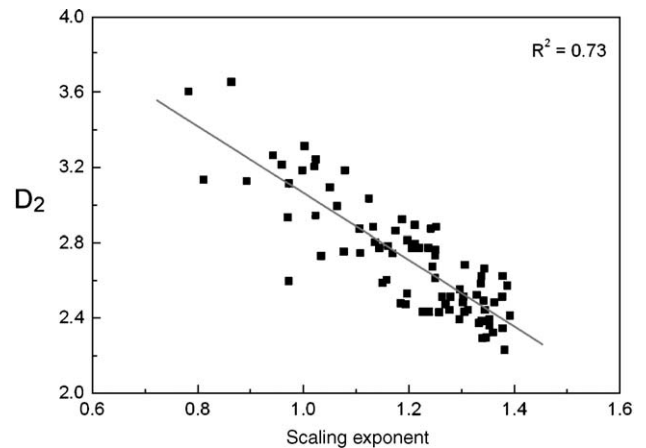


Fig. 5 – Negative correlation between the scaling exponent and the averaged correlation dimension plot ($n = 5$).

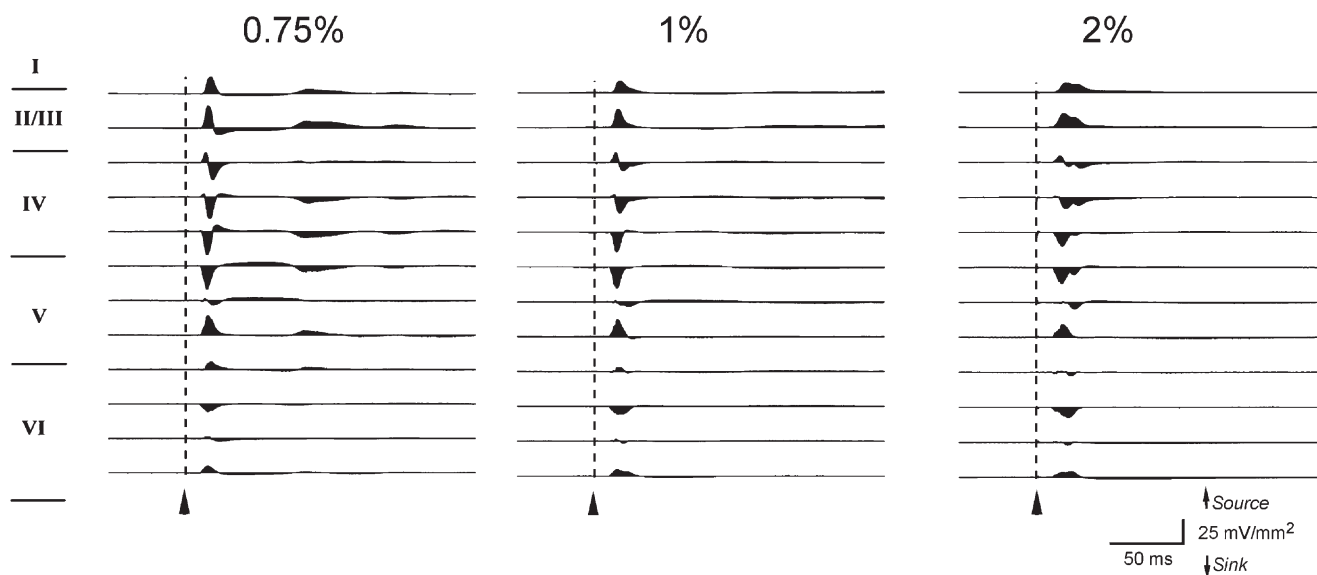
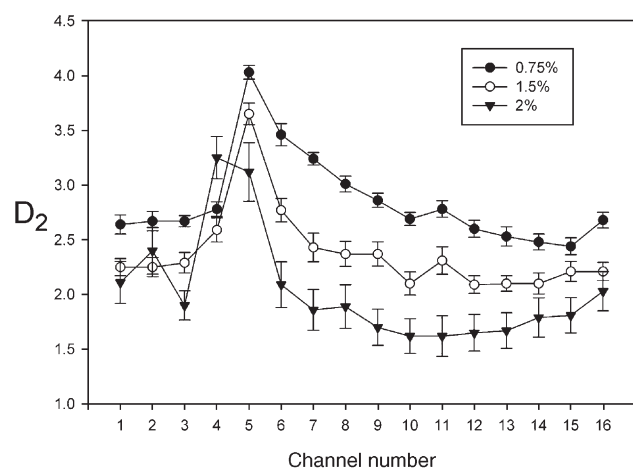
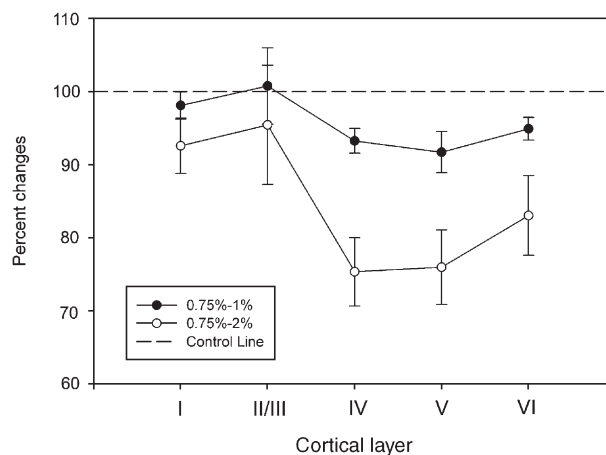
a Cortical evoked CSD under different halothane concentrations**b** Effect of the halothane of the D_2 in different channel**c** Halothane effect on D_2 of different cortical layers

Fig. 6 – The effect of halothane concentration on the evoked responses and the correlation dimension. **(a)** The amplitudes of the evoked CSD profiles under 0.75%, 1% and 2% halothane, respectively. The arrow heads indicate the stimulation onset. The vertical arrows indicate the direction of sink or source currents. **(b)** Example of halothane effects on intracortical D_2 in 16 channels. **(c)** Effects of increasing halothane, (0.75% to 1% and 0.75% to 2%) on the D_2 in the different cortical layers. Data were shown as mean and SEM ($n = 5$).

control values. The percent change of D_2 was calculated by dividing the 1% or 2% halothane D_2 value from each channel with that under the 0.75% halothane (control values). The channel values attributed to the different cortical layers were grouped and the results are shown in Fig. 6c. The percent decrease of D_2 as halothane concentration was increased was largest in layer IV, indicating that layer IV is the most sensitive to depth of anesthesia (Table 2).

A two-way repeated measures ANOVA with concentration and cortical layer as the within-subject variables ($F(4, 49) = 4.71$, $P < 0.02$) revealed that D_2 values differed significantly across cortical layers (Table 3). Moreover, there was a significant interaction between concentration and cortical

layer ($F(4, 49) = 11.70$, $P < 0.001$). Post hoc tests showed that the 2% halothane significantly depressed the activities of layers IV, V, and VI (P 's < 0.001) but not of layers I and II/III. The complexity of the layer IV was suppressed to 24.6% compared with the reduction of 7.5% of that in layer I when halothane increased from 0.75% to 2%.

2.5. Effects of VPL inactivation

To test the importance of the thalamic input drive on complexity, the thalamic VPL nucleus was temporarily inactivated. The experimental set up is shown in Fig. 7a. The accuracy of the microinjector placement was assessed by observing VPL thalamic unit activities after peripheral

Table 2 – D_2 percent changes in the cortical layers under 1% and 2% halothane

Cortical layers	D_2 (1%)/ D_2 (0.75%)	D_2 (2%)/ D_2 (0.75%)
I	0.981 ± 0.021	0.926 ± 0.042
II/III	1.007 ± 0.058	0.954 ± 0.091
IV	0.932 ± 0.019	0.753 ± 0.052
V	0.917 ± 0.031	0.759 ± 0.057
VI	0.949 ± 0.017	0.830 ± 0.061

Data are shown as means ± SEM (n = 5).

electrical stimulation (Fig. 7b, upper sweeps). Simultaneous multichannel EEG recording and the evoked CSD activation profiles of one typical example are plotted in Fig. 7b. Attenuation of thalamic and cortical responses was apparent after microinjection of 1 μ l of lidocaine into the VPL (Fig. 7b). Both thalamic and cortical evoked activities recovered by 30 min after the lidocaine injection. The extents of lidocaine diffusion for five subjects are delineated in Fig. 7a; note that the overlapped diffusion area (blackened) covered most of the VPL.

The D_2 data set were calculated from the spontaneous EEG signals obtained before, during and 30 min after the injection of lidocaine, and were plotted against the cortical layers (Fig. 7c). Two-way ANOVA showed that there were significant differences in layers and treatment conditions ($F(4, 39) = 49.61$, $P < 0.001$ and $F(2, 39) = 5.01$, $P < 0.05$, respectively, Table 4). Post hoc tests showed that there were significant differences in treatment conditions within layer IV (control vs. lidocaine treatment, $P = 0.017$ and lidocaine treatment vs. recovery, $P = 0.001$). There was a trend toward reduction of D_2 in layers II/III after lidocaine treatment.

3. Discussion

The present surrogate data provides strong evidence that nonlinearity is a significant feature of the primary somatosensory cortex, and that the underlying deterministic interaction loops in this region are likely to be revealed by examining their intra-cortical complexities using nonlinear methods. The present experimental findings are the first to our knowledge to measure correlation dimensions in simultaneously recorded cortical local field potentials. We observed that activities across the cortical layers had different D_2 values. Combining the sink source current profiles with histological examination enabled the cortical layers to be accurately located. The D_2 value of cortical layer IV was the largest, followed by layers II/III, V, and I and finally VI. Cortical layer-dependent complexity can be expressed by D_2 and the scaling exponent, and these two values are reversibly related. The D_2 of layer IV was reduced significantly by temporary inactivation of the VPL, and the effect was reversible as indicated by the recovery of the thalamic and cortical evoked responses. The complexity changes in different cortical layers were also sensitive to the changes of activity level regulated by halothane anesthesia.

The cortical recording sites in the present study were in the area that receives thalamic afferents relayed from the opposite hind limb. The structural basis of the cortical module in this part of the primary somatosensory cortex was also described recently (Skoglund et al., 2004). Their distinct organization of neurons and dendritic bundles in rodent primary somatosensory cortex provides the anatomical basis for cortical cell modules. The common inputs and close contact within the bundles and the reciprocal connections via both intra-areal lateral connections and inter-areal feedback/feedforward pathways enable these modules to work synchronously and to distribute coordinated signals widely across various cortical and subcortical areas.

From the observation of the spontaneous EEG we found that activities in layer IV differs substantially from the other layers and is most likely due to the fact that synaptic potentials generated from apical dendrites of infragranular pyramidal neurons tend to reverse polarity in this layer and are therefore greatly attenuated. Additionally, it is common to observe an abundance of high frequency activities in and around layer IV where multiunit activities were initiated from soma of spiny stellate neurons. The basis for the higher complexity and wider frequency band in the layer IV as found in the present study thus can be explained partly by the attenuation of post synaptic potentials and abundance of unit discharges in layer IV. Decreased afferent inputs by reversible deactivation of the VPL and increase the depth of anesthesia would both decrease in multiunit discharges, and thus decrease the D_2 value.

The polarity reversal above and below the layer IV reflects the existence of the vertically oriented current dipole of opposite and closely correlated polarity in the infra- and supragranular layers which was formed by the post synaptic potentials in the basal and apical dendrites of infragranular pyramidal neurons (Jellema et al., 2004). Thus it is reasonable to expect the linear or nonlinear activity to be highly correlated between these layers. The finding that complexity as reflected in D_2 were similar in layers II/III and V, may be due to the fact that spontaneous field potentials in these layers are generated by common post synaptic processes in dendrites of infragranular pyramidal neurons.

Estimation of the nonlinearity-based complexity using correlation dimension has revealed a large variation in the functional states of the brain. The nature of cortical nonlinearity, however, has remained unresolved. It has been proposed that a D_2 value is proportional to the number of independent components contained in a total system (Egolf and Greenside, 1994); and that systems with mixed feedback (positive and negative) and multiple feedback streams with different time constants are sources

Table 3 – ANOVA of correlation dimension of intracortical EEG by cortical layer and halothane concentration

D_2	Squares	df	Mean square	F	P
Layers, within groups	0.147	4	0.037	4.712	0.0161
Halothane, within groups	0.101	1	0.101	3.105	0.176
Layers × halothane	0.034	4	0.008	11.697	0.0004

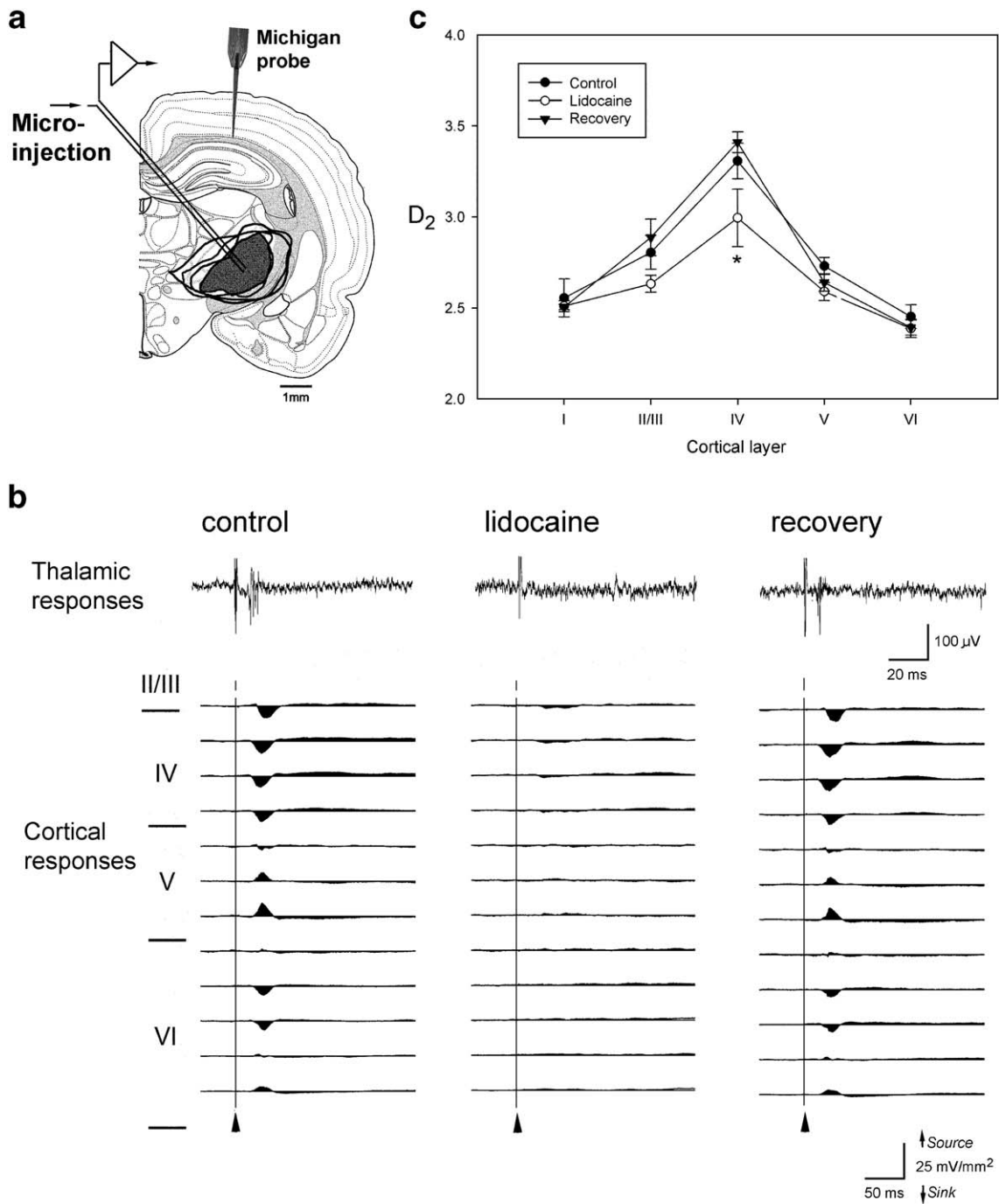


Fig. 7 – Reversible inactivation of thalamic activities and the effect of blocking thalamic input on cortical layer complexity. (a) Schematic diagram of the placement of recording-microinjection hybrid electrode, Michigan probe and the anatomical location of thalamic nuclei. The solid lines delineate the approximate diffusion range of the solution injected into the VPL thalamic nucleus in 4 different animals. The blackened area represents the overlapped areas. Note that the Michigan probe and hybrid electrode were not placed in the same coronal plane in the actual experimental setting. (b) Evoked response before, during and 30 min after microinjection of 1 μ l of lidocaine. A typical example of evoked thalamic and cortical GSD profile following the peripheral electrical stimulation is shown. The evoked thalamic unit activities are shown in the upper sweeps. Note that the thalamic unit responses were completely abolished and the sink currents across the layers were markedly reduced after the injection. Both of the effects were recovered almost completely within 30 min. The arrow heads indicate the stimulation onset. The vertical arrows indicate the direction of sink or source currents. (c) D_2 data were calculated and collected from spontaneous EEG signals before, during and 30 min after the injection of lidocaine in four different animals. D_2 values from histologically verified cortical layers were pooled. D_2 in layer IV only was significantly decreased after the injection. D_2 values 30 min after injection were not different from pre-injection values.

Table 4–The ANOVA of correlation dimension of the intracortical EEG from different cortical layers and treatment conditions

D_2	Squares	df	Mean square	F	P
Layers, within groups	4.657	4	1.164	49.611	<0.001
Conditions, within groups	0.235	2	0.118	5.014	0.012
Layers \times halothane	0.258	8	0.032	1.374	0.238

of chaos (Glass et al., 1987). Thus, one possible physiological implication of a D_2 measurement is that it may be an indirect indication of the quantity of independent circuit components. The finding of cortical layer-dependent complexity suggests that there is a differential distribution of the number of independent circuit components in each cortical layer. The high dynamical complexity in layer IV indicates that there are more independent circuit components this layer. The spiny stellate neurons in layer IV are the principle target of the thalamocortical axons as well as recurrent excitatory connection from other cells in the same layer (Martin, 2002; Peters and Kara, 1985a, 1987). This recurrent excitatory circuitry is controlled by both feedforward and feedback inhibition, which are mediated by distinct classes of inhibitory GABAergic interneurons (Kawaguchi and Kubota, 1997; Peters and Kara, 1985b). In highly recurrent layer IV network, the stabilization of neuronal network activities may be achieved through a coordinated set of changes in excitatory and inhibitory circuitry. The strength of recurrent excitation and feedback inhibition can be modulated by thalamic inputs. In turn the modulated changes in layer IV excitability in response to thalamic inputs may enhance the ability of layer IV to amplify the input signals it receive (Feldmeyer et al., 2002; Maffei et al., 2004; Stoop et al., 2002), thereby enhancing the signal to noise ratio.

The changes of D_2 across cortical layers could be attributed to changes in several of these independent circuit components reflected in the collective extra-cellular field potential and recorded by the electrodes in the respective layers. Our CSD analysis revealed that the earliest sink occurred in layer IV and then the currents sweep upward to layers II and III and downward to layers V and VI. This finding corroborates the recent experimental result of the electric-evoked sequential CSD pattern in rodent's primary somatosensory cortex (Jellema et al., 2004) and the current view of a basic neuronal circuit: that there is intracolumnar processing leading to different output channels and that cortical efferent neurons with different extrinsic targets are partially segregated, such that those of layers II/III project to other cortical areas, while those of layers V/VI project to subcortical structures (Douglas and Martin, 2004; Mountcastle, 1997). Thus it appears that the collective neuronal activities emerge from an ensemble of independently active assemblies in layer IV that transfer information flow to other layers. Consequently, this organization results in a synchronization of independently operating components into correlated activities. This synchronization may reduce the number of independent, autonomous components and thus yield a D_2 decrease.

Alternatively, the neurophysiological nature of the D_2 may be related to the frequency distribution of cortical oscillation. Different EEG frequencies have been associated with different functional brain states. Our findings showed that frequency distributions differ among the cortical layers and that the EEG spectrum of layer IV has the widest distribution of the layers tested. This wide distribution produces a distinctively low scaling exponent. The D_2 value is also a scaling measure of the system in its reconstructed phase space. The present scaling behavior findings of the complexity exponents D_2 and β are consistent with previous reports which have suggested that the brain may work in a highly nonlinear manner (Chen et al., 1997; Gilden et al., 1995; Linkenkaer-Hansen et al., 2001), and that as such its activity cannot be qualitatively and quantitatively characterized by simple observation with common linear methods. The increased D_2 in layer IV appears to be attributable to an upward frequency shift in the alpha, beta and gamma bands in the power spectrum and a power decrease in the low frequency range. As D_2 and β have been found to be negatively correlated, the D_2 decreases that we found in cortical layer IV in the presence of increased halothane concentration or thalamic inactivation were expected to produce a shift to a lower power in the high frequency range and an increase in the power of low frequency oscillation. The relationship between the scaling exponent and the correlation dimension make it possible to use D_2 variation to estimate spectrum distribution.

The wide distribution of the frequency bands in cortical layer IV reflects the extensive interplay of the extrinsic thalamocortical inputs on the intrinsic cortical spontaneous dynamics. Although the existence of fast and slow cortical oscillations has long been known to be an important feature of EEG activity, the corresponding cellular mechanisms of the widely distributed oscillation in neocortex have only begun to be unraveled in recent years. It has been demonstrated that the low-threshold burst spikes evoked by activation of thalamocortical relay neurons activate cortical layer IV neurons. The excitation of these cortical neurons causes feedback re-excitation in the thalamocortical projection neurons via reciprocal connections between the two neuronal groups (McCormick and Bal, 1997). Thus, fast oscillations are generated in thalamic and cortical circuits as the result of these reciprocal interactions (Steriade and Deschenes, 1984). The variability of oscillatory patterns (slow oscillation, spindles and delta) that characterizes the state of quiet sleep was also promoted by the corticothalamic system acting as a complex network (Amzica and Steriade, 2000).

It has been suggested that cortical synchronizations of neuronal assemblies occurring in the high frequency range may be controlled directly by ascending cholinergic and serotonergic inputs to the neocortex (Dringenberg and Vanderwolf, 1998). And thalamic reticular neurons have been shown to be inhibited by cholinergic projections from the brainstem reticular core and basal forebrain (Steriade and McCarley, 2005). In this respect, the occurrence of a shift from a high to a low frequency range in layer IV during thalamic deactivation and halothane treatment suggests that there is a neuromodulatory control mechanism that drives brain activity away from an adaptive state and enables the brain to accommodate wide spread changes.

In the present study, the averaged D_2 of each layer was uniformly decreased with increasing halothane concentrations. A similar effect of gas anesthesia on D_2 was recently reported (Widman et al., 2000). Neuronal activity was suppressed progressively with increases in anesthetic depth, as evidenced by examining the evoked sink source patterns. The tendency for layer dependent D_2 results persisted even under a high halothane concentration, and the maximal loss of complexity was found in layer IV under a very high anesthesia level. Although the brain's excitatory state was assumed to be suppressed non-specifically by the inhalation of the halothane, there is evidence from a functional brain imaging study suggesting that the essential common neurophysiological mechanism underlying halothane-induced unconsciousness may be a hyperpolarization block of thalamocortical neurons (Alkire et al., 2000). On the other hand, a recent electrophysiological study showed that halothane can antagonize the occurrence of fast oscillations in the cortex and even block seizures (Grenier et al., 2003). Halothane may exert a more specific attenuation of the electrical interactions at gap junctions between cortical neurons, which generate synchronized high frequency activity. Thus, the halothane effect on the complexity of cortical layer IV may be mediated by its specific actions on the extrinsic thalamocortical pathways and intrinsic cortical circuit elements.

Different approaches, such as bispectral index, AAI™ index and EEG entropy, have been developed to monitor depth of anesthesia in a clinic setting. However, there is still controversy regarding the predictive value of these methods for the individual, due to questions about response linearity and inter-individual variation (Anderson et al., 2003; Anderson and Jakobsson, 2004; Muncaster et al., 2003; Rampil et al., 1998). Although our aim was not to improve clinical monitoring of anesthetic depth, more studies examining intra-cortical complexity in different brain regions under different anesthetic agents, anesthetic dosage versus response profiles, and non-invasive techniques to detect the deep cortical potentials would be informative in this regard. Our study did demonstrate that intracortical activities may be a more sensitive index of brain functional states than surface EEG.

4. Experimental procedures

4.1. Experimental animals

Male Sprague–Dawley rats (National Laboratory Animal Center, Taipei, Taiwan, ROC) weighing 250–350 g were used. Rats were housed with an artificial light system, under a 12 h light/dark cycle, at 22 °C. The rats had free access to food and water. All experiments were carried out in accordance with the National Institutes Guide for the Care and Use of Laboratory Animals, and approved by, the Academia Sinica Institutional Animal Care and Utilization Committee. All efforts were made to minimize animal suffering and to use a minimal number of animals.

4.2. Animal preparation

Rats were anesthetized with halothane (2–3% in 30%/70% nitrous oxide/oxygen mixture) and placed in a small animal

stereotaxic frame in preparation for surgery. Rats' rectal temperatures were measured and maintained at ≥ 36.5 °C via a homeothermo blanket system (Harvard apparatus, USA). A PE-240 tube was inserted into the tracheal via tracheotomy through which the rats could voluntarily inhale the halothane and oxygen gas mixture. The electrocardiogram was recorded on an oscilloscope and CO₂ concentration was monitored (Normpcap 200 oxy, Detax Instrumentarium Corp., Finland) and maintained within the range of 3–4%. Concentrations of inhaled halothane (0–2 minimum alveolar concentration) were monitored continuously using a calibrated infrared gas analyzer (Capnomac Ultima, Datex Ohmeda, Helsinki, Finland). The rat's skull was exposed and holes were drilled to allow electrodes access to the left primary somatosensory cortex or thalamic nucleus. Electric stimulation (0.1 ms, 1 mA square wave constant current) was applied to the right hind paw from a pulse generator (Model 2100, A–M Systems, Inc., USA) via two stainless steel wires.

4.3. Recording and data acquisition

Surface cortical field potentials evoked by electrical stimulation were recorded by a tungsten electrode and systemically mapped on the hind limb projection area in the primary somatosensory cortex. A 16-channel (1 × 16) Michigan probe was then positioned to the recording site where the largest evoked field potential amplitude had been obtained. The inter-contact lead distance on the probe was 150 μm . The recording depth ranged from the cortical surface to 2250 μm deep, enabling evoked and spontaneous EEG signals of cortical layers I to VI to be monitored simultaneously. One Ag–AgCl reference electrode was placed beneath the scalp. Analog EEG signals were amplified by a 16-channel amplifier (Medusa Digital BioAmp, TDT Inc., USA) and passed through a 0.1 Hz to 7.5 KHz analog bandpass filter. Evoked and spontaneous EEG signals were sampled at a rate of 250 Hz and digitized to 12 bits precision using a DSP data acquisition system based on PC system (TDT Inc., USA). The signal sampling frequency is 5 to 10 time higher than the unfiltered signal bandwidth. Thus, the EEG signals are adequately sampled and suitable for data analysis.

4.4. Reversible deactivation of VPL thalamic nucleus

The location of the left VPL thalamic nucleus was functionally identified by recording the thalamic responses to electrical stimulation of the right hind paw. A hybrid electrode combining a recording tungsten electrode and microinjection micro-tube (20 μm ID, 90 μm OD, MicroFil, WPI Inc., USA) was constructed. The micro-tube was filled with 2% lidocaine (Xylocaine, AstraZeneca, Sweden) and connected to a perfusion pump. This recording-microinjection electrode was inserted with a 40 degree angle of insertion relative to the right cortex and lowered into the left VPL. The point of insertion was 3.0 mm posterior and 2.0 mm lateral (right) to bregma. Thalamic activities were monitored and examined as the recording electrode advanced and electrical stimulation pulses were applied to the right hind paw. The electrode was fixed at the location where the short latency thalamic unit responses were recorded. To deactivate the thalamic

responses, 1 μ l of 2% lidocaine was infused into the VPL for 2 min. The inhibitory effect of the lidocaine and the recovery of the thalamic responses to the electrical stimulation were monitored continuously.

4.5. Alteration of the general brain state in variant halothane concentration

Three concentrations, 0.75%, 1% and 2%, were employed to establish the general background activities. Inhaled halothane (0–2 minimum alveolar concentration) was monitored continuously using a calibrated infrared gas analyzer. At least 5 min was allowed after changing halothane concentration to maintain a stable condition for multichannel EEG signal recording. The rat's heart rate and reflex activity were monitored and tested periodically during the recording session.

4.6. Current source density

The field potentials evoked by the electrical stimulation was recorded for 1 s (6000 points) per trial. Twenty trials of evoked field potentials were averaged for each channel. To accurately locate the synaptic currents mediating the local extracellular potentials, the 16 channels of averaged field potentials were subjected to a one-dimensional, three-point current source density (CSD) analysis formula (Freeman and Nicholson, 1975; Mitzdorf, 1985). The CSD of channel n , I_n , was derived from the second spatial derivation of the averaged field potentials, ϕ , according to the following equation:

$$I_n = (1/4h^2) * (\phi(x - 2h) - 2\phi(x) + \phi(x + 2h))$$

where $h = 150 \mu\text{m}$ is the distance between channels, and x is the coordinate of each channel. The spatial profiles of current sinks and sources along the axis of the electrode were evaluated. The data averaged over the 10 ms before stimulation onset was chosen as baseline. Current density values less than the baseline value were designated as current sinks, assuming an inward directed current; values larger than the baseline were designated as current sources.

4.7. Nonlinear analysis

The data analysis program was based on the Nonlinear Time Series Analysis (TISEAN) subprograms (in C language) written by Hegger et al. (1999). The main program was constructed in MATLAB. Eight-second epochs (sampling rate 250 Hz; 2000 points) of spontaneous EEG data were used for data analysis. Takens' delay embedding theorem (Takens, 1981) was used to reconstruct the phase space of an attractor. Phase portraits were constructed by expanding a single scalar time series $\{x_1, \dots, x_i, \dots, x_N\}$ into m -dimensional vectors, $\vec{X}_i = (x_{i-(m-1)\tau}, x_{i-(m-2)\tau}, \dots, x_i)$ where $i = 1 + (m-1)\tau, \dots, N-1, N$ and τ denotes the time lag. The first local minimum of mutual information of the scalar time series estimated the time lag τ (Fraser and Swinney, 1986) and the false nearest neighbor method was used to determine the minimal sufficient embedding dimension m . In our data, m was around 4–6, and τ was approximately 80 ms. The D_2 was estimated by using

the Grassberger and Procaccia's algorithm (Grassberger and Procaccia, 1983). The correlation sum of a given phase portrait in phase space is defined as

$$C(r) = \frac{2}{N_p(N_p - 1)} \sum_{i=1}^{N_p} \sum_{j=i+1}^{N_p} \theta(r - |\vec{X}_i - \vec{X}_j|)$$

where θ is the Heaviside step function and N_p is the total number of points of the phase portrait. Since $C(r) \propto r^{D_2}$, the linear slope of $\log C(r)$ versus $\log r$ plot gives the estimated D_2 for the scaling region. In order to get $D_{2,i}$ for each EEG data $\vec{X}_i(t)$, values of $(C(r_s), r_s)$ were calculated where $s = 1, 2, \dots, k$ and $r_{s+1} - r_s = \frac{(r_k - r_1)}{k-1} > 0$. And $D_{2,i}^j$ was defined as the linear regression slope of $\log C(r_{j+l})$ versus r_{j+l} where $l = 1, 2, \dots, 5$ and $j = 1, 2, \dots, k-4$. Linear regression slopes were obtained from every successive 5 points along the plot and a histogram was constructed based on these slope values. The final value of $D_{2,i}$ was obtained by selecting the bin number (bin width = 0.01) of the histogram of $D_{2,i}^j$ that has the maximum occurrence. The D_2 obtained by averaging 15 subsets among each 120 s recording period of each channel represented the dimensional complexity of each channel across the cortical layers.

4.8. Surrogate data analysis

In the present study a nonlinear analysis tool was used to obtain the correlation dimension D_2 as the indicator to the dimensional complexity of the EEG signals. However, it has been reported that nonlinear algorithms can mistake linear correlations for determinism in time series data (Grassberger, 1987; Nicolis and Nicolis, 1984), in particular those of the power law type (Osborne and Provenzale, 1989; Theiler, 1991). Thus, it is important to test for nonlinearities hidden in the EEG signals, before subjecting the data to nonlinear methods of analysis. The idea is to test results against the null hypothesis of a specific class of linear random processes, e.g., the Gaussian linear stochastic process. One of the most popular of such tests is the method of "surrogate data" (Schreiber and Schmitz, 1996), which can be used with any nonlinear statistic that characterizes a time series by a single number. According to Schreiber and Schmitz's methods (Schreiber and Schmitz, 1996), the number of signals of our EEG data for each surrogate is 2000 with the discrepancy between 0.000012 and 0.0224. In the present investigation, the surrogate data and its corresponding values of correlation dimension were both obtained from the original EEG signals using the TISEAN (Schreiber and Schmitz, 1996).

4.9. Power spectrum analysis

The power spectrum density computed from Fast Fourier Transform of different frequency bands was also analyzed. It included low frequency (1–8 Hz), alpha (8–12.5 Hz), Beta (12–30 Hz), and Gamma (40–70 Hz) bands. The scaling exponent, β was obtained from linear regression fit of log-log power spectrum plot within a frequency range of 2–70 Hz.

4.10. Statistics

The test of nonlinearity was carried out by Wilcoxon matched-pairs signed-rank test comparing pairs of D_2 values calculated

on the original data sets and their corresponding surrogate data sets. Mean data values are presented with their standard deviations. The D_2 and scaling exponent values from different cortical layers and different groups were compared using ANOVA. Two-way ANOVA was used to analyze the effects of different halothane concentrations and thalamic deactivation on the D_2 values from different cortical layers. Tukey's post hoc test was used to detect the sources of significant comparisons.

4.11. Methods

Once the rats were fully prepared, evoked field potential by electrical stimulation of the contralateral hind paw were recorded and the CSD method was applied to characterize the current sources and sinks along the channels. Spontaneous EEG signals were recorded continuously for 160 s. Both linear and nonlinear time series analysis methods were applied. The anesthesia level was changed by adjusting the concentration of halothane (0.75%, 1% or 2%). The same recording process was repeated before and after each concentration change. The effects of thalamic deactivation were then investigated in 4 rats and the multichannel EEG signals were sampled before, immediately and 30 min after the injection of 2% lidocaine into the functionally identified VPL thalamic nucleus.

4.12. Histology

To verify the recording loci, a small lesion was made by passing a DC anodal current (30 μ A for 5 s) to the 16th contact lead (the deepest electrode on the probe) at the conclusion of the experiment. A second lesion was made at the same lead after the Michigan probe was withdrawn 1000 μ m. In the selective thalamic deactivation experiment, the recording-microinjection hybrid electrode was withdrawal from the brain and then the lidocaine in the micropipette was replaced with pontamine sky blue (Sigma, USA, 2% dissolved in 0.9% saline). After re-insertion of the hybrid electrode into the VPL site, 1 μ l of sky blue was infused into the VPL to mark the injection site and for estimation of the approximate diffusion area of the lidocaine. The brains were cut into 60- μ m thick coronal sections using a cryostat and the sections were stained with cresyl violet (Sigma, USA). Drawings of the sections with clear electrode tracks and lesion marks were made. The cortical layers were identified by inspecting neuronal shapes under a light microscope. Swanson's rat atlas (Swanson, 1992) was used as reference in the histological identification of structures.

Acknowledgments

We are most thankful to Dr. Richard Hahnloser, ETHZNIZH, Switzerland, for many helpful suggestions and comments. Multichannel silicon probes were provided by the University of Michigan Center for Neural Communication Technology sponsored by NIH NIBIB grant P41-RR09754. This study was supported by grants from the National Science Council and the Academia Sinica, Taiwan, ROC.

REFERENCES

- Alkire, M.T., Haier, R.J., Fallon, J.H., 2000. Toward a unified theory of narcosis: brain imaging evidence for a thalamocortical switch as the neurophysiologic basis of anesthetic-induced unconsciousness. *Cogn.* 9, 370–386.
- Amzica, F., Steriade, M., 2000. Integration of low-frequency sleep oscillations in corticothalamic networks. *Acta Neurobiol. Exp.* 60, 229–245.
- Anderson, R.E., Jakobsson, J.G., 2004. Entropy of EEG during anaesthetic induction: a comparative study with propofol or nitrous oxide as sole agent. *Br. J. Anaesth.* 92, 167–170.
- Anderson, R.E., Barr, G., Assareh, H., Jakobsson, J., 2003. The AAI index, the BIS index and end-tidal concentration during wash in and wash out of sevoflurane. *Anaesthesia* 58, 531–535.
- Anokhin, A.P., Birbaumer, N., Lutzenberger, W., Nikolaev, A., Vogel, F., 1996. Age increases brain complexity. *Electroencephalogr. Clin. Neurophysiol.* 99, 63–68.
- Babloyantz, A., Destexhe, A., 1986. Low dimensional chaos in an instance of epileptic seizure. *Proc. Natl. Acad. Sci. U. S. A.* 83, 3513–3517.
- Babloyantz, A., Salazar, J.M., Nicolls, C., 1985. Evidence of chaotic dynamics of brain activity during the sleep cycle. *Phys. Lett. A* 111, 152–156.
- Chen, Y., Ding, M., Scott Kelso, J.A., 1997. Long memory processes (1/f alpha type) in human coordination. *Phys. Rev. Lett.* 79, 4501–4504.
- Crick, F., Koch, C., 1998. Constraints on cortical and thalamic projections: the no-strong-loops hypothesis. *Nature* 391, 245–250.
- Douglas, R.J., Martin, K.A., 2004. Neuronal circuits of the neocortex. *Annu. Rev. Neurosci.* 27, 251–419.
- Dringenberg, H.C., Vanderwolf, C.H., 1998. Involvement of direct and indirect pathways in electrocorticographic activation. *Neurosci. Biobehav. Rev.* 22, 243–257.
- Egolf, D.A., Greenside, H.S., 1994. Relation between fractal dimension and spatial correlation length for extensive chaos. *Nature* 369, 129–131.
- Feldmeyer, D., Lubke, J., Silver, R.A., Sakmann, B., 2002. Synaptic connections between layer 4 spiny neurone-layer 2/3 pyramidal cell pairs in juvenile rat barrel cortex: physiology and anatomy of interlaminar signalling within a cortical column. *J. Physiol.* 538, 803–822.
- Ferri, R., Elia, M., Musumeci, S.A., Stam, C.J., 2001. Non-linear EEG analysis in children with epilepsy and electrical status epilepticus during slow-wave sleep (ESES). *Clin. Neurophysiol.* 112, 2274–2280.
- Fraser, A.M., Swinney, H.L., 1986. Independent coordinates for strange attractors from mutual information. *Phys. Rev. A* 33, 1134–1140.
- Freeman, J.A., Nicholson, C., 1975. Experimental optimization of current source density technique for anuran cerebellum. *J. Neurophysiol.* 38, 369–382.
- Gilden, D.L., Thornton, T., Mallon, M.W., 1995. 1/f noise in human cognition. *Science* 267, 1837–1839.
- Glass, L., Guevara, M.R., Shrier, A., 1987. Universal bifurcations and the classification of cardiac arrhythmias. *Ann. N. Y. Acad. Sci.* 584, 168–178.
- Grassberger, P., 1987. Evidence for climatic attractors. *Nature* 326, 524.
- Grassberger, P., Procaccia, I., 1983. Measuring the strangeness of strange attractors. *Physica D* 9, 189–208.
- Grenier, F., Timofeev, I., Steriade, M., 2003. Neocortical very fast oscillations (ripples, 80–200 Hz) during seizures: intracellular correlates. *J. Neurophysiol.* 89, 841–852.
- Hegger, R., Kantz, H., Schreiber, T., 1999. Practical implementation of nonlinear time series methods: the TISEAN package. *CHAOS* 9, 413–435.

- Jellema, T., Brunia, C.H., Wadman, W.J., 2004. Sequential activation of microcircuits underlying somatosensory-evoked potentials in rat neocortex. *Neuroscience* 129, 283–295.
- Jeong, J., Kim, S.Y., Han, S.H., 1998. Nonlinear dynamical analysis of the EEG in Alzheimer's disease with optimal embedding dimension. *Electroencephalogr. Clin. Neurophysiol.* 106, 220–228.
- Jones, E.G., 2000. Microcolumns in the cerebral cortex. *Proc. Natl. Acad. Sci. U. S. A.* 97, 5019–5021.
- Kantz, H., Schreiber, T., 1997. *Nonlinear Time Series Analysis*. Cambridge Univ. Press.
- Kawaguchi, Y., Kubota, Y., 1997. GABAergic cell subtypes and their synaptic connections in rat frontal cortex. *Cereb. Cortex* 7, 476–486.
- Kotini, A., Anninos, P., 2002. Detection of non-linearity in schizophrenic patients using magnetoencephalography. *Brain Topogr.* 15, 107–113.
- Lee, Y.-J., Zhu, Y.-S., Xu, Y.-H., Shen, M.-F., Zhang, H.-X., Thakor, N. V., 2001. Detection of non-linearity in the EEG of schizophrenic patients. *Clin. Neurophysiol.* 112, 1288–1294.
- Lehnertz, K., 1999. Nonlinear time series analysis of intracranial EEG recordings in patients with epilepsy—An overview. *Int. J. Psychophysiol.* 34, 45–52.
- Linkenkaer-Hansen, K., Nikouline, V.V., Palva, J.M., Ilmoniemi, R.J., 2001. Long-range temporal correlations and scaling behavior in human brain oscillations. *J. Neurosci.* 21, 1370–1377.
- Maffei, A., Nelson, S.B., Turrigiano, G.G., 2004. Selective reconfiguration of layer 4 visual cortical circuitry by visual deprivation. *Nat. Neurosci.* 7, 1353–1359.
- Martin, K.A., 2002. Microcircuits in visual cortex. *Curr. Opin. Neurobiol.* 12, 418–425.
- McCormick, D.A., Bal, T., 1997. Sleep and arousal: thalamocortical mechanisms. *Annu. Rev. Neurosci.* 20, 185–215.
- Mitzdorf, U., 1985. Current source-density method and application in cat cerebral cortex: investigation of evoked potentials and EEG phenomena. *Physiol. Rev.* 65, 37–100.
- Mountcastle, V.B., 1997. The columnar organization of the neocortex. *Brain* 120, 701–722.
- Mountcastle, V.B., 2003. Introduction. *Computation in cortical columns. Cereb. Cortex* 13, 2–4.
- Muncaster, A.R., Sleight, J.W., Williams, M., 2003. Changes in consciousness, conceptual memory, and quantitative electroencephalographical measures during recovery from sevoflurane- and remifentanyl-based anesthesia. *Anesth. Analg.* 96, 720–725.
- Nicolis, C., Nicolis, G., 1984. Is there a climatic attractor? *Nature* 311, 529–532.
- Osborne, A.R., Provenzale, A., 1989. Finite correlation dimension for stochastic systems with power-law spectra. *Physica D* 35, 357–381.
- Pereda, E., Gamundi, A., Nicolau, M.C., Rial, R., Gonzalez, J., 1999. Interhemispheric differences in awake and sleep human EEG: a comparison between non-linear and spectral measures. *Neurosci. Lett.* 263, 37–40.
- Peters, A., Kara, D.A., 1985a. The neuronal composition of area 17 of rat visual cortex: I. The pyramidal cells. *J. Comp. Neurol.* 234, 218–241.
- Peters, A., Kara, D.A., 1985b. The neuronal composition of area 17 of rat visual cortex: II. The nonpyramidal cells. *J. Comp. Neurol.* 234, 242–263.
- Peters, A., Kara, D.A., 1987. The neuronal composition of area 17 of rat visual cortex: IV. The organization of pyramidal cells. *J. Comp. Neurol.* 260, 573–590.
- Rampil, I.J., Kim, J.S., Lenhardt, R., Negishi, C., Sessler, D.I., 1998. Bispectral EEG index during nitrous oxide administration. *Anesthesiology* 89, 671–677.
- Scannell, J.W., Burns, G.A., Hilgetag, C.C., O'Neil, M.A., Young, M.P., 1999. The connective organization of the cortico-thalamic system of the cat. *Cereb. Cortex* 9, 277–299.
- Schreiber, T., Schmitz, A., 1996. Improved surrogate data for nonlinearity tests. *Phys. Rev. Lett.* 77, 635–638.
- Skoglund, T.S., Pascher, R., Berthold, C.H., 2004. Aspects of the organization of neurons and dendritic bundles in primary somatosensory cortex of the rat. *Neurosci. Res.* 50, 189–198.
- Stam, C.J., Jelles, B., Achtereekte, H.A., Rombouts, S.A., Slaets, J.P., Keunen, R.W., 1995. Investigation of EEG non-linearity in dementia and Parkinson's disease. *Electroencephalogr. Clin. Neurophysiol.* 95, 309–317.
- Steriade, M., Deschenes, M., 1984. The thalamus as a neuronal oscillator. *Brain Res.* 320, 1–63.
- Steriade, M., McCarley, R.W., 2005. *Brain Control of Waking and Sleep*, 2nd ed. Klüver-Plenum.
- Stoop, R., Blank, D., Kern, A., v d Vyver, J.J., Christen, M., Lecchini, S., Wagner, C., 2002. Collective bursting in layer IV. Synchronization by small thalamic inputs and recurrent connections. *Cogn. Brain Res.* 13, 293–304.
- Swanson, L.W., 1992. *Brain Maps: Structure of the Rat Brain*. Elsevier, Amsterdam.
- Takens, F., 1981. Detecting Strange Attractors in Turbulence, *Lecture Notes in Math*, vol. 898. Springer-Verlag, New York.
- Theiler, J., 1991. Some comments on the correlation dimension of $1/f\alpha$ noise. *Phys. Lett. A* 155, 480–483.
- Theiler, J., 1995. On the evidence for low-dimensional chaos in an epileptic electroencephalogram. *Phys. Lett. A* 196, 335–341.
- Van Cappellen van Walsum, A.M., Pijnenburg, Y.A., Berendse, H. W., van Dijk, B.W., Knol, D.L., Scheltens, P., Stam, C.J., 2003. A neural complexity measure applied to MEG data in Alzheimer's disease. *Clin. Neurophysiol.* 114, 1034–1040.
- Van der Heyden, M.J., Velis, D.N., Hoekstra, B.P.T., Pijn, J.P.M., van Emde Boas, W., van Veelen, C.W.M., van Rijen, P.C., Lopes da Silva, F.H., DeGoede, J., 1999. Non-linear analysis of intracranial human EEG in temporal lobe epilepsy. *Clin. Neurophysiol.* 110, 1726–1740.
- Widman, G., Schreiber, T., Rehberg, B., Hoefl, A., Elger, C.E., 2000. Quantification of depth of anesthesia by nonlinear time series analysis of brain electrical activity. *Phys. Rev. E* 62, 4898–4903.